

## Raman properties of gold nanoparticle-decorated individual carbon nanotubes

Tilman Assmus, Kannan Balasubramanian, and Marko Burghard<sup>a)</sup>

Max-Planck-Institut für Festkörperforschung, Heisenbergstr. 1, 70569 Stuttgart, Germany

Klaus Kern

Max-Planck-Institut für Festkörperforschung, Heisenbergstr. 1, 70569 Stuttgart, Germany

and Institut de Physique des Nanostructures, Ecole Polytechnique Fédérale de Lausanne (EPFL), CH-1015 Lausanne, Switzerland

Matteo Scolari, Nan Fu, Anton Myalitsin, and Alf Mews

Universität Siegen, Adolf Reichwein Str. 2, 57068 Siegen, Germany

(Received 20 February 2007; accepted 26 March 2007; published online 24 April 2007)

Single-wall carbon nanotubes decorated by gold nanoparticles with sizes of a few tens of nanometers were investigated by confocal Raman microscopy. It was found that individual nanoparticles impart a sizable Raman enhancement exceeding one order of magnitude, without appreciably interfering with polarization dependent Raman measurements. By contrast, cavity effects within small nanoparticle agglomerates resulted in a 20-fold stronger enhancement and significant distortions of the polarization characteristic. © 2007 American Institute of Physics.

[DOI: 10.1063/1.2731662]

Raman spectroscopy has been proven to be a highly versatile tool to probe the vibrational and electronic properties of carbon nanotubes (CNTs).<sup>1–3</sup> A number of Raman studies on CNTs have taken advantage of the surface enhancement by local optical fields of silver or gold nanostructures.<sup>4</sup> In fact, the first Raman spectra of individual single-wall nanotubes (SWCNTs) have been obtained with the aid of a rough silver film substrate.<sup>5</sup> In surface enhanced Raman spectroscopy (SERS), the Raman signal can be amplified by up to 14 orders of magnitude (om's), which allows studying single molecules.<sup>6,7</sup>

SERS studies of CNTs have revealed intriguing effects such as anomalies of the Stokes to anti-Stokes ratio and power exchange between different phonon modes.<sup>8</sup> The SERS effect can significantly alter the symmetries of the excited vibrations in CNTs.<sup>9</sup> For pristine nanotubes, theory predicts  $A_1$  symmetry for the radial breathing mode (RBM), while the  $G$ -line is composed of up to six modes with  $E_1$ ,  $E_2$ , and  $A_1$  symmetry.<sup>10,11</sup> By experiment, the  $A_1$  symmetry of the RBM could so far be observed only indirectly by determining the ratio  $\bar{\alpha}^2/\gamma_s^2$  from the tensor invariants of the Raman tensor in backscattering configuration ( $\bar{\alpha}^2$ : isotropic part,  $\gamma_s^2$ : symmetric anisotropy),<sup>12</sup> whereas its direct verification has been hampered by the depolarization effect.<sup>13</sup> For the  $G$ -line, components of  $A_1$  and  $E_2$  symmetry have been identified by their polarization dependence.<sup>14</sup> Based upon the samples investigated so far, the extent to which the enhancement affects the Raman scattering properties of CNTs has been difficult to evaluate.<sup>9</sup> In this letter, we present SERS data collected from individual SWCNTs that have been partially decorated by gold nanoparticles (NPs) via an electrodeposition method, enabling us to compare the polarization dependence of the important Raman modes for different NP arrangements.

Single-walled carbon nanotubes were synthesized on Si/SiO<sub>2</sub> (100 nm thermal oxide) substrates by chemical vapor deposition (CVD) using Fe nanoparticles as catalyst. AuPd electrodes were then deposited using e-beam lithography. Electrodeposition of gold NPs onto the tubes was accomplished using an electrodeposition bath consisting of an aqueous solution (pH 2) containing 2 mM KAuCl<sub>4</sub>, 0.1 mM LiClO<sub>4</sub>, and 5 mM polyvinylpyrrolidone K30 as surface stabilizing agent. By adjusting the electrodeposition potential and time, gold NPs with sizes between 10 and 100 nm were formed on the nanotubes. The modified nanotubes were characterized by atomic force microscopy (AFM) and diffraction-limited micro-Raman spectroscopy utilizing circularly polarized light with  $\lambda_{\text{exc}}=568$  nm and a power of 500  $\mu\text{W}$ . The samples were first examined by scanning confocal Raman imaging and, subsequently, local spectra were acquired by a charge coupled device in spectroscopy mode. All spectra were normalized to the substrate Raman peak at 520  $\text{cm}^{-1}$ . In the vicinity of a gold NP we frequently observed a pronounced  $D$  band, which we attribute to a preferential NP nucleation at defect sites.<sup>15</sup> For polarization dependent experiments, two polarizers were added to the setup, as described in Ref. 13.

In Fig. 1, the Raman spectrum collected over an isolated NP (size of  $\sim 40$  nm) on top of a SWCNT is displayed. Based on the plot of Kataura *et al.*,<sup>16,17</sup> the measured RBM position  $\omega_{\text{RBM}}=161$   $\text{cm}^{-1}$  and the used excitation wavelength ( $\lambda_{\text{exc}}=568$  nm), this SWCNT is tentatively assigned to the semiconducting (15,7) tube. The presence of a semiconducting tube is corroborated by the absence of a Breit-Wigner-Fano (BWF) resonance within the  $G$  line, and the observation, that nanotubes with  $\nu=(n-m) \bmod 3=-1$  have a higher Raman cross section than other tubes.<sup>17</sup> Compared to the bare segment on the same tube, the presence of the NP causes an increase of the RBM and  $G$ -line intensity by a factor of  $\sim 4$ . In order to compare this to enhancement factors for molecules, as reported in the literature,<sup>6,18</sup> it has to be taken into account that the local electromagnetic field from

<sup>a)</sup>Electronic mail: m.burghard@fkf.mpg.de

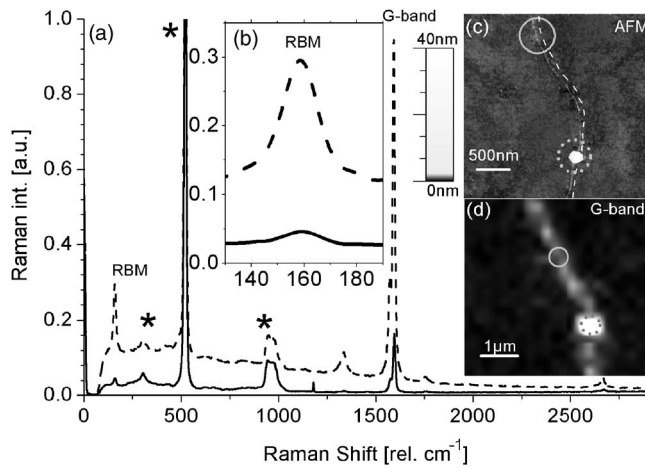


FIG. 1. Raman spectra recorded at two positions (circles) along a SWCNT (NT1). (a) Comparison between the spectra taken on the bare tube (solid line) and over a gold particle deposited onto the tube (dashed line) reveals an enhancement of the *G* line and RBM by a factor of  $\sim 4$ . Substrate peaks are labeled by \*. (b) Magnified spectra in the RBM range. (c) AFM image of the investigated tube. The location of the nanotube has been highlighted by a dashed line. (d) Raman *G*-line image of the particle-decorated tube segment.

surface plasmons decays very rapidly from the NP surface. Accordingly, the Raman signal is only enhanced for molecules in the range of just a few nanometers from the particle surface. Assuming that only a few % of the CNT within the diffraction limited laser spot ( $d \approx 500$  nm) is enhanced by the NP, the local enhancement would be two to three  $\text{om}'s$ , consistent with theory.<sup>19</sup>

Raman spectra acquired from another SWCNT, decorated with a small agglomeration of gold NPs, are presented in Fig. 2. Using the plot of Kataura *et al.* from Refs. 16 and 17, the measured RBM position  $\omega_{\text{RBM}} = 221 \text{ cm}^{-1}$  and  $\lambda_{\text{exc}} = 568$  nm, this SWCNT is assigned to the metallic (13,1) tube. The broadened *G* line displayed by this nanotube is indicative of a BWF resonance, and consistent with a metallic character. The effective Raman intensity increase is found to be approximately three  $\text{om}'s$  upon particle decoration.

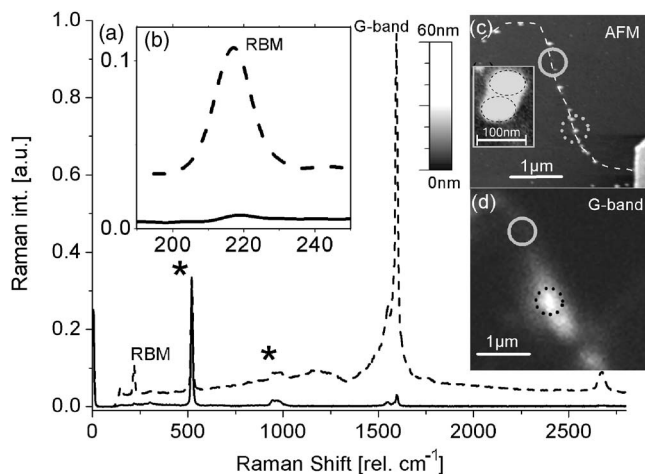


FIG. 2. (a) Raman spectra of a second SWCNT (NT2), acquired on a bare tube section (solid line) and above an agglomeration of several gold NPs (dashed line). Substrate peaks are labeled by \*. In the enhanced spectrum, the *G* line and RBM (b) appear with two  $\text{om}'s$  increased intensity. (c) AFM image of the nanotube with a scanning electron microscopy inset of the agglomeration. The nanotube is highlighted by a dashed line. (d) *G*-line Raman image used to localize the CNT's bare and modified regions.

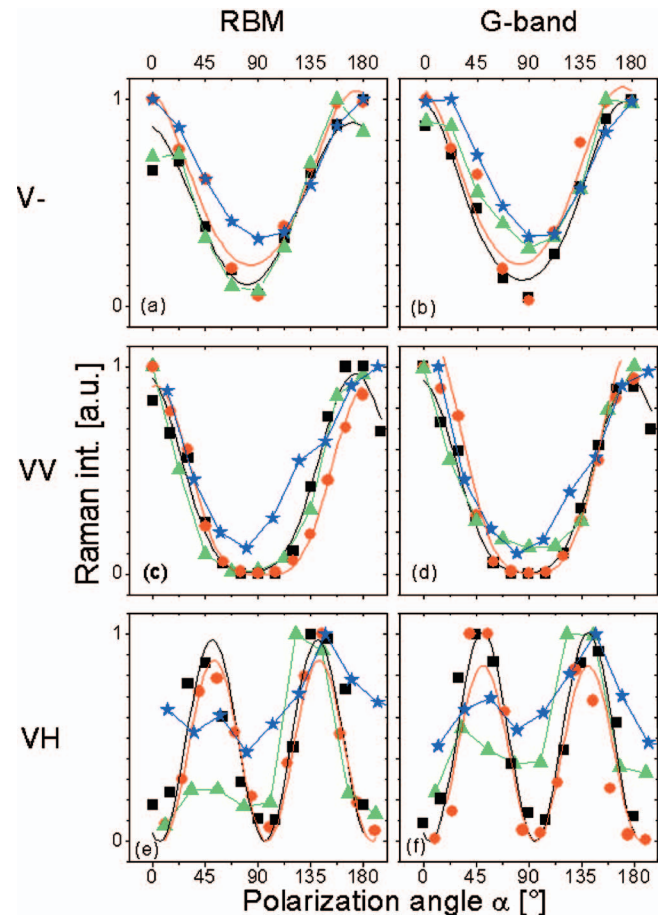


FIG. 3. (Color) Normalized polarization dependence of the RBM and *G*-line intensity measured on NT1 and NT2. For NT1, the bare tube (black  $\blacksquare$ ) is compared with a section modified by a single gold NP (red  $\bullet$ ). The NT2 spectra were acquired above two different gold NP agglomerations (green  $\blacktriangle$  and blue  $\blackstar$ ) on the nanotube, which differ in the geometrical arrangement of the particles. For NT1 (black and red), the solid lines are fits to the dependencies expected by theory, whereas for NT2 (green and blue) a straight connection of the data points is presented, since there is no model available.

Several other SWCNTs decorated by NP agglomerates of similar size yielded enhancement factors between one and four  $\text{om}'s$ , independently of the electronic properties of the tubes. This observation is in accordance with the existence of enhanced electromagnetic fields inside cavities formed between NPs with a separation of the order of a few nanometers.<sup>20</sup> For instance, from electromagnetic theories it is predicted that the enhancement in the center of particle dimers with an interparticle distance of just a few nanometers can be several  $\text{om}'s$  higher than at the surface of individual particles, albeit they are also very sensitive to the geometry of the aggregate.<sup>19</sup>

The number and arrangement of the NPs on the tubes exerted a profound influence on the Raman response, as apparent from Fig. 3, which plots the polarization angle dependence of RBM and *G* line (maximum intensity component at  $1590 \text{ cm}^{-1}$ ) for the SWCNTs of Figs. 1 and 2. It is noteworthy that the other components of the *G* line (at  $1570$  and  $1550 \text{ cm}^{-1}$ ) showed similar behavior as the  $1590 \text{ cm}^{-1}$  component. We first address NT1 that bears an isolated NP. The data gained in (V-) configuration [Figs. 3(a) and 3(b)] provide evidence that the tube absorbs most strongly when the polarization vector of the incoming light is parallel to the tube axis, independent of the presence of the NP. This finding

reflects the well-documented antenna effect of CNTs.<sup>21</sup> In the (VV) configuration [Figs. 3(c) and 3(d)], the bare NT1 displays a  $\cos(\alpha)^4$  dependence of the Raman intensity, as expected from theory. Similar agreement with the theory exists in case of the (VH) configuration, for which a  $\cos(\alpha)^2 \sin(\alpha)^2$  dependence is observed [Figs. 3(e) and 3(f)]. Essentially the same dependencies can be discerned over the NP, despite the 40-fold Raman enhancement that it generates. Such a negligible influence on the polarization dependence was found for all investigated isolated NPs on different SWCNTs. This observation demonstrates, that the single particle induces an isotropic SERS effect with the field component along the tube axis enhancing the absorption and hence the Raman cross section of the tube. In contrast, for the two different NP agglomerations on NT2, a clear tendency to absorb light also when the polarization is perpendicular to the tube axis can be seen in the (V-) [Figs. 3(a) and 3(b)] and (VV) configurations [Figs. 3(c) and 3(d)], i.e., the Raman intensity does not approach zero for  $\alpha=90^\circ$ . Even more pronounced differences are apparent from the data collected in the (VH) configuration, as manifested by a pronounced flattening of the angular dependence for both agglomerates [Figs. 3(e) and 3(f)]. Especially the second aggregate (blue stars) displays an almost complete loss of the characteristic angular dependence. This behavior indicates that the measured polarization dependence is predominantly dictated by the electromagnetic enhancement governed by the geometry of the NP agglomerates. In fact, gold NP agglomerates such as the present ones can have a complex electromagnetic near-field distribution with a strong preferential orientation as well as only a tiny angular dependence.<sup>22</sup>

In conclusion, we directly observed the symmetries of the important Raman modes of individual SWCNTs decorated by gold nanoparticles. This sample configuration enabled us to study the dependence of both the Raman enhancement magnitude and the extent to which polarization-dependent measurements are affected, on the nanoparticle arrangement. Further valuable information can be expected from experiments that allow for a more detailed structural

characterization of the CNT/NP-hybrid systems, which could be achieved by, e.g., transmission electron microscopy.

The authors thank the DFG for financial support (Grant Nos. BU1125/3 and ME1380/9).

- <sup>1</sup>A. Mews, F. Koberling, T. Basche, G. Philipp, G. S. Duesberg, S. Roth, and M. Burghard, *Adv. Mater. (Weinheim, Ger.)* **12**, 1210 (2000).
- <sup>2</sup>A. Jorio, R. Saito, J. H. Hafner, C. M. Lieber, M. Hunter, T. McClure, G. Dresselhaus, and M. S. Dresselhaus, *Phys. Rev. Lett.* **86**, 1118 (2001).
- <sup>3</sup>A. Hartschuh, E. J. Sanchez, X. S. Xie, and L. Novotny, *Phys. Rev. Lett.* **90**, 9 (2003).
- <sup>4</sup>K. Kneipp, H. Kneipp, M. S. Dresselhaus, and S. Lefrant, *Philos. Trans. R. Soc. London, Ser. A* **362**, 2361 (2004).
- <sup>5</sup>G. S. Duesberg, W. J. Blau, H. J. Byrne, J. Muster, M. Burghard, and S. Roth, *Chem. Phys. Lett.* **310**, 8 (1999).
- <sup>6</sup>S. M. Nie and S. R. Emery, *Science* **275**, 1102 (1997).
- <sup>7</sup>M. Moskovits, *Rev. Mod. Phys.* **57**, 783 (1985).
- <sup>8</sup>K. Kneipp, L. T. Perelman, H. Kneipp, V. Backman, A. Jorio, G. Dresselhaus, and M. S. Dresselhaus, *Phys. Rev. B* **63**, 19 (2001).
- <sup>9</sup>K. Kneipp, A. Jorio, H. Kneipp, S. D. M. Brown, K. Shafer, J. Motz, R. Saito, G. Dresselhaus, and M. S. Dresselhaus, *Phys. Rev. B* **63**, 8 (2001).
- <sup>10</sup>A. Jorio, M. A. Pimenta, A. G. Souza, R. Saito, G. Dresselhaus, and M. S. Dresselhaus, *New J. Phys.* **5**, 139 (2003).
- <sup>11</sup>A. Kasuya, Y. Sasaki, Y. Saito, K. Tohji, and Y. Nishina, *Phys. Rev. Lett.* **78**, 4434 (1997).
- <sup>12</sup>S. Reich and C. Thomsen, *Phys. Rev. Lett.* **85**, 3544 (2000).
- <sup>13</sup>G. S. Duesberg, I. Loa, M. Burghard, K. Syassen, and S. Roth, *Phys. Rev. Lett.* **85**, 5436 (2000).
- <sup>14</sup>A. Jorio, M. A. Pimenta, C. Fantini, M. Souza, A. G. Souza, G. G. Samsonidze, G. Dresselhaus, M. S. Dresselhaus, and R. Saito, *Carbon* **42**, 1067 (2004).
- <sup>15</sup>Y. W. Fan, M. Burghard, and K. Kern, *Adv. Mater. (Weinheim, Ger.)* **14**, 130 (2002).
- <sup>16</sup>H. Kataura, Y. Kumazawa, Y. Maniwa, I. Umezumi, S. Suzuki, Y. Ohtsuka, and Y. Achiba, *Synth. Met.* **103**, 2555 (1999).
- <sup>17</sup>C. Thomsen, H. Telg, J. Maultzsch, and S. Reich, *Phys. Status Solidi B* **242**, 1802 (2005).
- <sup>18</sup>K. Kneipp, Y. Wang, H. Kneipp, L. T. Perelman, I. Itzkan, R. Dasari, and M. S. Feld, *Phys. Rev. Lett.* **78**, 1667 (1997).
- <sup>19</sup>H. X. Xu, J. Aizpurua, M. Käll, and P. Apell, *Phys. Rev. E* **62**, 4318 (2000).
- <sup>20</sup>K. Kneipp, H. Kneipp, and J. Kneipp, *Acc. Chem. Res.* **39**, 443 (2006).
- <sup>21</sup>A. Jorio, A. G. Souza, V. W. Brar, A. K. Swan, M. S. Unlu, B. B. Goldberg, A. Righi, J. H. Hafner, C. M. Lieber, R. Saito, G. Dresselhaus, and G. Dresselhaus, *Phys. Rev. B* **65**, 12 (2002).
- <sup>22</sup>H. X. Xu and M. Käll, *ChemPhysChem* **4**, 1001 (2003).